A CLOSED-FORM SOLUTION FOR A CRACK APPROACHING AN INTERFACE

Boris Nuller, Michael Ryvkin and Alexander Chudnovsky

A CLOSED-FORM SOLUTION FOR A CRACK APPROACHING AN INTERFACE

BORIS NULLER, MICHAEL RYVKIN AND ALEXANDER CHUDNOVSKY

A closed-form solution is presented for the stress distribution in two perfectly bonded isotropic elastic half-planes, one of which includes a fully imbedded semi-infinite crack perpendicular to the interface. The solution is obtained in quadratures by means of the Wiener–Hopf–Jones method. It is based on the residue expansion of the contour integrals using the roots of the Zak–Williams characteristic equation. The closed-form solution offers a way to derive the Green's function expressions for the stresses and the SIF (stress intensity factor) in a form convenient for computation. A quantitative characterization of the SIF for various combinations of elastic properties is presented in the form of function the $c(\alpha, \beta)$, where α and β represent the Dundurs parameters. Together with tabulated $c(\alpha, \beta)$ the Green's function provides a practical tool for the solution of crack-interface interaction problems with arbitrarily distributed Mode I loading. Furthermore, in order to characterize the stability of a crack approaching the interface, a new *interface parameter* χ, is introduced, which is a simple combination of the shear moduli μ_s and Poisson's ratios ν_s ($s = 1, 2$) of materials on both sides of the interface. It is shown that χ uniquely determines the asymptotic behavior of the SIF and, consequently, the crack stability. An estimation of the interface parameter prior to detailed computations is proposed for a qualitative evaluation of the crack-interface interaction. The propagation of a stable crack towards the interface with a vanishing SIF is considered separately. Because in this case the fracture toughness approach to the material failure is unsuitable an analysis of the complete stress distribution is required.

1. Introduction

Determining the stress field in the vicinity of a crack tip approaching a bimaterial interface has important applications for layered elastic materials. Zak and Williams [1963] proposed the first formulation and solution of the problem for a semi-infinite crack perpendicular to a bimaterial interface with the crack tip at the interface. Khrapkov [1968] offered a closed-form solution for the problem of a finite crack with its tip at the interface. Cook and Erdogan [1972] and Erdogan and Biricikoglu [1973] derived the integral equations and provided the numerical solutions for fully imbedded semi-infinite and finite cracks, and for cracks either terminating at or crossing the material interface. A similar dislocation approach was employed by [Wang and Stahle 1998] for the study of stress fields in the vicinity of a finite crack approaching the interface. Using the exact solution obtained for Mode III as a prototype, Atkinson [1975] introduced an asymptotic solution for the SIF with respect to a small distance ε between the crack tip and the interface. Here the SIF is presented as $K_I = \varepsilon^{p_1 - 1/2} f(\alpha, \beta)$, with p_1, α, and β representing the first root of the Zak–Williams characteristic equation and the Dundurs parameters respectively. Later, He and Hutchinson [1989] considered a set of more general problems related to crack arrest and to penetration through or deflected by the interface.

Employing the amplitude factor k_1 for the boundary value problem with a crack terminating at the interface, He and Hutchinson were able to improve the representation of K_I to

$$K_I = k_1 \varepsilon^{p_1 - 1/2} c(\alpha, \beta),$$

where the function $c(\alpha, \beta)$ is a solution of a system of singular integral equations. Romeo and Ballarini [1995] evaluated the function $c(\alpha, \beta)$ and applied the results to finite and semi-infinite cracks. For certain values of α and β, however, the evaluation of the function $c(\alpha, \beta)$ results in an uncertainty of $0 \cdot \infty$ type that cannot be resolved numerically. Leguillon et al. [2000] investigated of the competition between three fracture scenarios – primary crack growth, interface debonding, and a new crack nucleation beyond the interface – by means of asymptotic analysis.

In this paper we construct a closed-form solution for the problem of a semi-infinite crack perpendicular to an interface between two isotropic elastic half-planes under Mode I loading by the Winner–Hopf–Jones method [Noble 1958]. While Nuller et al. [2001] summarized some of the results earlier, here we present the complete solution along with an analysis of the closed-form representation of the function $c(\alpha, \beta)$. For convenience of application, the values of the function $c(\alpha, \beta)$ are computed and reported in Table 2. Romeo and Ballarini's results coincide with the closed-form solution only in the case when $\alpha = \beta = 0$ and diverge significantly when α approaches ± 1.

In Section 2 we present the general formulation and closed-form solution of an auxiliary problem on a crack fully imbedded in the left half-plane and perpendicular to the interface, which is conjugate (the same Wiener–Hopf equation) to the problem considered by [Khrapkov 1968]. Using this solution in Section 3, we evaluate the Green's function for the SIF. Section 4 is dedicated to an assessment of crack stability through an analysis of the asymptotic expression of the SIF. We introduce a new parameter of the interface, χ, to characterize the stability of a crack approaching the interface. The parameter χ is a simple combination of shear moduli and Poisson's ratios on both sides of the interface. Addressed separately is the case of stable crack propagation when the SIF concept of fracture mechanics does not apply.

The first root of the Zak–Williams characteristic equation p_1 is a cornerstone of crack stability analysis and, as such, of the asymptotic representations of the solution. A proof of the existence and uniqueness of the p_1 value in the strip $0 < \text{Re } p < 1$ of the complex plane of the Mellin transform parameter p for all possible values of elastic constants is presented in Appendix A. The dependence of the first root location on the real axis upon the interface parameter χ is also analyzed there.

2. General formulation

Consider a semi-infinite crack perpendicular to the interface between two perfectly bonded dissimilar elastic half-planes Figure 1. The distance of the crack tip from the interface is ε. The elastic properties of the materials are defined by the shear moduli μ_s and Poisson's ratio's ν_s. The values of the index $s = 1, 2$ correspond to the uncracked and the cracked half-planes respectively. We introduce the system of polar coordinates R, θ in which the origin lies at the intersection of the crack axis and the interface such that the crack is located along the line $\theta = \pi$. Formulating the problem with the non-dimensional radial coordinate $r = R/\varepsilon$, the crack tip is associated with the point $r = 1$, $\theta = \pi$.
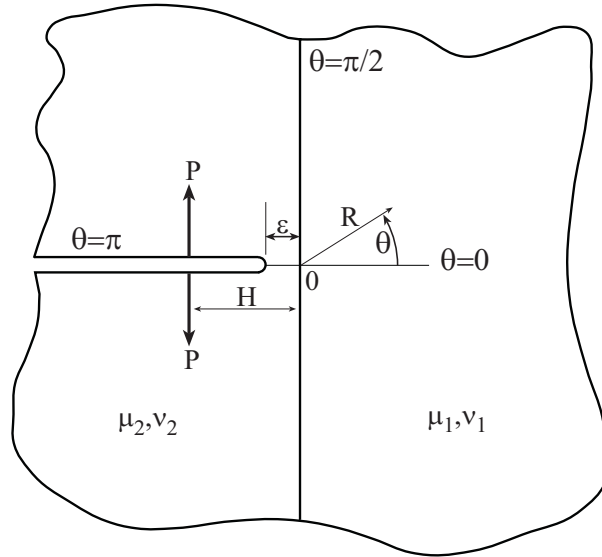
Figure 1. Perpendicular to the interface crack, fully imbedded in the left half-plane.

We assume that the loading corresponds to the Mode I, the stress field vanishes at $r \to \infty$, and the the local strain energy is bounded in the crack tip vicinity. Using the apparent symmetry, we formulate the boundary value problem for the upper half-plane $0 < \theta < \pi$, $0 < r < \infty$ as follows. The radial and angular displacements $u(r, \theta)$, $v(r, \theta)$ and the stresses $\sigma_\theta(r, \theta)$ satisfy the continuity conditions at the interface

$$[v(r, \pi/2)] = [u(r, \pi/2)] = 0; \qquad [\sigma_\theta(r, \pi/2)] = [\tau_{r\theta}(r, \pi/2)] = 0, \quad 0 < r < \infty, \tag{1}$$

where $[f(r, \theta)]$ denotes the jump of $f(r, \theta)$ in the θ direction. At the boundary of the half-plane

$$v(r, 0) = 0, \qquad \tau_{r\theta}(r, 0) = \tau_{r\theta}(r, \pi) = 0, \qquad 0 < r < \infty, \tag{2}$$

$$v(r, \pi) = v(r), \qquad 0 < r \le 1, \tag{3}$$

$$\sigma_\theta(r, \pi) = \sigma(r), \qquad 1 < r < \infty. \tag{4}$$

Here the function $\sigma(r)$ represents the applied load and $v(r) \equiv 0$ for the problem under consideration. However, we write condition in Equation (3) in a more general form for future consideration. We seek the solution as Papkovich–Neuber functions presented in the form of the Mellin integrals

$$2\mu_s v(r, \theta) = \frac{1}{2\pi i} \int_{L_0} [A_s(p)(p - \kappa_s) \sin(p+1)\theta + B_s(p)(p-1) \sin(p-1)\theta +$$
$$+ C_s(p)(p - \kappa_s) \cos(p+1)\theta + D_s(p)(p-1) \cos(p-1)\theta] r^{-p} dp, \tag{5}$$

$$2\mu_s u(r, \theta) = \frac{1}{2\pi i} \int_{L_0} [A_s(p)(p + \kappa_s) \cos(p+1)\theta + B_s(p)(p-1) \cos(p-1)\theta -$$
$$- C_s(p)(p + \kappa_s) \sin(p+1)\theta - D_s(p)(p-1) \sin(p-1)\theta] r^{-p} dp, \tag{6}$$

where the integration path L_0 is a contour parallel to the imaginary axis of the plane of the complex Mellin transform parameter p, and $\kappa_s = 3 - 4\nu_s$. The subscript $s = 1, 2$ denotes the quantities related to the right ($0 < \theta < \pi/2$) and left ($\pi/2 < \theta < \pi$) quadrants respectively. The unknown functions A_s, B_s, C_s, D_s are to be defined from the boundary conditions.

Using Jones method [Noble 1958] we introduce "−" and "+" transforms

$$v^-(p) = \int_1^\infty v(r, \pi) r^{p-1} dr, \qquad \sigma^+(p) = \int_0^1 \sigma_\theta(r, \pi) r^p dr,$$

which are analytical in the respective left and right half-planes separated by the contour L_0. Other functions analytical in these half-planes will be also denoted by the superscripts "+" and "−". The boundary conditions given by Equations (3) and (4) may now be presented as

$$v(r, \pi) = \frac{1}{2\pi i} \int_{L_0} [v^-(p) + v^+(p)] r^{-p} dp, \qquad 0 < r < \infty \tag{7}$$

$$\sigma_\theta(r, \pi) = \frac{1}{2\pi i} \int_{L_0} [\sigma^-(p) + \sigma^+(p)] r^{-p-1} dp, \qquad 0 < r < \infty \tag{8}$$

$$\sigma^-(p) = \int_1^\infty \sigma(r) r^p dr, \qquad v^+(p) = \int_0^1 v(r) r^{p-1} dr. \tag{9}$$

Substitution of Equations (5) and (6) into the boundary conditions in Equations (1), (2), (7) and in Equations (1), (2), (8) yields two systems of eight linear algebraic equations, each with coefficients $a_{ik}(p)$ with respect to the unknowns $A_1(p), B_1(p), ..., D_2(p)$. In both systems the first seven equations are identical and homogeneous. The only nonhomogeneous equations are the last ones obtained from conditions in Equations (7) and (8). Denoting the determinants of the first and second systems as $N_v(p)$ and $N_\sigma(p)$ respectively, the expression for the function $A_1(p)$ may be presented in the following alternative forms

$$A_1(p) = \frac{[v^-(p) + v^+(p)] M(p)}{N_v(p)}, \qquad A_1(p) = \frac{[\sigma^-(p) + \sigma^+(p)] M(p)}{N_\sigma(p)}, \tag{10}$$

where $M(p)$ is the cofactor of the element $a_{81}(p)$, which is the same in both systems, and where

$$N_v(p) = \mu_2^{-1} b_0 b_1 b_2 (1-p)^2 \sin^2 \pi p, \qquad N_\sigma(p) = 2p(1-p)^2 \sin \pi p N(p), \tag{11}$$

$$N(p) = 2b_1(b_2 \cos \pi p + b_3 p^2) + b_4, \tag{12}$$

where

$$b_0 = 1 + \kappa_2, \qquad b_1 = 1 + \kappa_1 \mu, \qquad b_2 = \mu + \kappa_2, \, b_3 = 2(\mu - 1),$$

$$b_4 = -2\kappa_1 \mu^2 - (\kappa_1 - 1)(\kappa_2 - 1)\mu + \kappa_2^2 + 1, \qquad \mu = \frac{\mu_2}{\mu_1}.$$

Equating the right hand sides of Equations (10) we obtain the Wiener–Hopf equation

$$\sigma^- + \sigma^+ = K(p)[v^-(p) + v^+(p)], \qquad K(p) = \frac{N_\sigma(p)}{N_v(p)}, \quad p \in L_0, \tag{13}$$

for the two unknown functions $\sigma^+(p)$ and $v^-(p)$. The solution is constructed using the technique developed by [Nuller 1976]. The function $K(p)$ can be presented in the form of a product $K(p) = K_1(p) K_2(p)$,

where

$$K_1(p) = 4\mu_2 b_0^{-1} p \cot \pi p \,, \qquad K_2(p) = \frac{2b_1(b_2 \cos \pi p + b_3 p^2) + b_4}{2b_1 b_2 \cos \pi p}.$$

Factorization with respect to the contour L_0, which is taken to be the imaginary axis, yields

$$K_m(p) = \frac{K_m^+(p)}{K_m^-(p)} \,, \qquad m = 1, 2.$$

For the function $K_1(p)$, the factorization is trivial. For the function $K_2(p)$ the factorization is carried out by the use of the Cauchy-type integrals, see [Gakhov 1966] and can be performed due to the following properties of this function on L_0: (1) it is Hölder continuous; (2) it has no zeros, see Appendix A; (3) it has zero index; and (4) $\ln K_2(p)$ decays exponentially as $|p| \to \infty$, which follows from the asymptotic relation $K_2(it) \sim 1 + O[t^2 \exp(-\pi |t|)]$, as $|t| \to \infty$. Hence, the factorization $K(p) = K^+(p)[K^-(p)]^{-1}$ is given by

$$
\begin{aligned}
K^+(p) &= \frac{4\mu_2 \Gamma(p+1)}{b_0 \Gamma(p+1/2)} K_2^+(p), \\[6pt]
K^-(p) &= \frac{\Gamma(1/2-p)}{\Gamma(1-p)} K_2^-(p) \,, \\[6pt]
K_2^\pm(p) &= \exp\left[-\frac{1}{2\pi i} \int_{-i\infty}^{i\infty} \frac{\ln K_2(t) dt}{t-p} \right], \qquad p \bar{\in} L_0 \\[6pt]
K_2^\pm(p) &= K_2^{\pm 1/2}(p) \exp\left[-\frac{1}{2\pi i} \int_{-i\infty}^{i\infty} \frac{\ln K_2(t) dt}{t-p} \right], \qquad p \in L_0,
\end{aligned}
\tag{14}
$$

where $\Gamma(p)$ is the Gamma function.

Now the Wiener–Hopf Equation (13) can be rewritten in the following form

$$\frac{\sigma^-(p) + \sigma^+(p)}{K^+(p)} = \frac{v^-(p) + v^+(p)}{K^-(p)}, \qquad p \in L_0. \tag{15}$$

Let the external conditions be given by the power form expressions

$$\sigma(r) = a r^{-\gamma-1} \,, \qquad v(r) = b r^\delta, \tag{16}$$

with $\gamma > 0$, $\delta > 0$, and $a < 0$, which corresponds to Mode I loading. For this case Equations (9) yield

$$\sigma^-(p) = \frac{-a}{p-\gamma} \,, \qquad v^+(p) = \frac{b}{p+\delta} \,, \tag{17}$$

and the nonhomogeneous Wiener–Hopf Equation (15) can be factorized as follows

$$
\begin{aligned}
\frac{\sigma^+(p)}{K^+(p)} + \frac{a}{p-\gamma}\left[\frac{1}{K^+(\gamma)} - \frac{1}{K^+(p)} \right] - \frac{b}{(p+\delta)K^-(-\delta)} = \\[6pt]
\frac{v^-(p)}{K^-(p)} + \frac{b}{p+\delta}\left[\frac{1}{K^-(p)} - \frac{1}{K^-(-\delta)} \right] + \frac{a}{(p-\gamma)K^+(\gamma)}. \tag{18}
\end{aligned}
$$

Both parts of the last equality are analytical in their respective half-planes separated by the contour L_0 and decrease at least as p^{-1} or faster when $|p| \to \infty$. Employing now Liouville's theorem, we conclude

that each side of Equation (18) is equal to zero. Consequently, we find the stress transform to be

$$\sigma^+(p) = K^+(p)\left[\frac{b}{(p+\delta)K^-(-\delta)} - \frac{a}{(p-\gamma)K^+(\gamma)}\right] + \frac{a}{p-\gamma} . \tag{19}$$

The asymptotic stress distribution at the crack tip is defined by the stress transform behavior for large $|p|$. From Equations (14) and (19) it is evident that for $|p| \to \infty$

$$\sigma^+(p) \sim -\frac{4\mu_2}{1+\kappa_2}\left[\frac{a}{K^+(\gamma)} - \frac{b}{K^-(-\delta)}\right]p^{-1/2} . \tag{20}$$

As a result,

$$\sigma_\theta(r,\pi) \sim -\frac{4\mu_2}{1+\kappa_2}\left[\frac{a}{K^+(\gamma)} - \frac{b}{K^-(-\delta)}\right]\frac{1}{\sqrt{\pi(1-r)}} , \qquad r \to 1-0 .$$

In view of the accepted length scale normalization, the actual displacements $v(R)$ are obtained from the scaled displacements derived in the solution by multiplying by ε, that is, $v(R) = \varepsilon v(r)$. Consequently, the relation between the scaled and the non-scaled stresses is

$$\sigma(R,\theta) = \frac{\sigma(r,\theta)}{\varepsilon} . \tag{21}$$

3. Green's function for SIF

The study of crack stability near the interface requires solutions for arbitrarily distributed loads, which can be obtained using the Green's function of the particular problem, namely the solution for the two unit forces $P = 1$ applied to the crack faces symmetrically at some point $R = H$; see Figure 1. This solution is defined by the boundary conditions in Equations (1), (2) and (4) with

$$\sigma_\theta(r) = -\delta(r-h) ,$$

where $\delta(r)$ is the delta function and $h = H/\varepsilon$.

Through the superposition principle this problem may be considered as the sum of the following two problems. The first is the problem seen in Equations (1), (2) and (4) with $\sigma_\theta(r) = -\delta(r-h)$ for $0 < r < \infty$. The second is a mixed problem defined by the conditions given in Equations (1)–(4) with $\sigma(r) = 0$ and $v(r) = -v_\delta(r)$, where $v_\delta(r)$ represents the displacements obtained in the first problem. The solution of the first problem clearly has no singularity at the point of interest $r = 1$, $\theta = \pi$ as the stresses $\sigma(r,\theta)$ are equal to zero for $0 < r < 1$. Therefore the singularity at this point for the Green's function of the initial problem is completely defined by the stress field of the second problem.

In the first problem the transforms of the applied loading are given by $\sigma^+(p) = 0$, and $\sigma^-(p) = -h^p$. Consequently, from Equations (10) and (11) we obtain

$$v_\delta(r) = -\frac{1}{2\pi i}\int_{L_0}\frac{Q(p)h^p}{N(p)r^p}dp, \qquad Q(p) = \frac{b_0 b_1 b_2 \sin\pi p}{2p\mu_2} .$$

Employing the residue theorem and closing the integration path to the left of the contour L_0 we find that for $r < 1$

$$v_\delta(r) = \sum_{k=1}^{\infty}\frac{Q(-p_k)r^{p_k}}{N'(-p_k)h^{p_k}} . \tag{22}$$

Here $p = -p_k$ are the roots of the Zak–Williams characteristic equation, see Equation (12):

$$N(p) = 0 \tag{23}$$

which are located in the left half-plane Re $p < 0$. The numbering is in accord with the increasing distance from the imaginary axis.

It follows from Equations (9), (16), (17), and (22) that for the second problem

$$v_\delta^+(p) = -\sum_{k=1}^{\infty} \frac{Q(-p_k)}{N(-p_k)(p + p_k)h^{p_k}} .$$

Taking into account that $\sigma^-(p) = 0$ and reapplying the procedure (17)–(20), we obtain

$$\sigma^+(p) \sim 2b_1 b_2 \left[\sum_{k=1}^{\infty} \frac{\sin \pi p_k}{p_k N'(-p_k) K^-(-p_k) h^{p_k}} \right] p^{-1/2}, \qquad |p| \to \infty . \tag{24}$$

Consequently, the asymptote of the singular stresses in the initial problem that also defines the Green's function for the SIF K_I is given by

$$\sigma_\theta(r, \pi) \sim 2b_1 b_2 \left[\sum_{k=1}^{\infty} \frac{\sin \pi p_k}{p_k N'(-p_k) K^-(-p_k) h^{p_k}} \right] \frac{1}{\sqrt{\pi(1-r)}}, \qquad r \to 1-0 . \tag{25}$$

The Cauchy-type integral representing the function $K^-(-p_k)$ converges exponentially. The series in the brackets of Equation (25) has the same type of convergence due to the multiplier h^{-p_k} and because the remaining terms have the order $O(\sqrt{p_k})$. The values p_k can be found from the characteristic equation (23) by the Newton's method using the asymptotics

$$p_k = k \pm i \frac{2}{\pi} \ln k + O(1)$$

for large k. In order to obtain the non-scaled form of the above result we have to replace r and h by R/ε and H/ε respectively and use the relation in Equation (21).

An asymptotic expression for the SIF Green's function for the problem at hand proceeds from the asymptotic representation given by Equation (25) of the hoop stress component:

$$K_I = c(\alpha, \beta) H^{-p_1} \varepsilon^{p_1 - 1/2} . \tag{26}$$

Here $c(\alpha, \beta)$ is a smooth and finite function of the Dundurs parameters α and β:

$$c(\alpha, \beta) = \frac{2\sqrt{2} b_1 b_2 \sin \pi p_1}{p_1 N'(-p_1) K^-(-p_1)} , \tag{27}$$

$$\alpha = \frac{\mu(\kappa_1 + 1) - \kappa_2 - 1}{\mu(\kappa_1 + 1) + \kappa_2 + 1} , \qquad \beta = \frac{\mu(\kappa_1 - 1) - \kappa_2 + 1}{\mu(\kappa_1 + 1) + \kappa_2 + 1} .$$

When $\varepsilon \to 0$, the SIF K_I apparently behaves as $\varepsilon^{p_1 - 1/2}$ and, depending on the value of p_1, tends to 0 or ∞. The values of the first root $p_1(\alpha, \beta)$ and the function $c(\alpha, \beta)$ for various combinations of α and β are presented in Tables 1 and 2. From these values the asymptote of the SIF for arbitrary material parameters combination can be obtained by interpolation. The values of p_1 agree with the graphical

$\alpha \setminus \beta$	−0.45	−0.4	−0.3	−0.2	−0.1	0.0	0.1	0.2	0.3	0.4	0.45
−0.95	0.872	0.803	0.717	0.661	0.622	0.592					
−0.9	0.868	0.799	0.713	0.657	0.618	0.589					
−0.8		0.789	0.704	0.650	0.611	0.583					
−0.7		0.777	0.694	0.641	0.604	0.576					
−0.6		0.764	0.683	0.631	0.5951	0.568	0.548				
−0.5			0.670	0.621	0.586	0.560	0.540				
−0.4			0.656	0.609	0.575	0.550	0.532				
−0.3			0.641	0.595	0.563	0.540	0.522				
−0.2			0.624	0.580	0.550	0.528	0.512	0.5			
−0.1				0.564	0.535	0.515	0.5	0.489			
0.0				0.545	0.519	0.5	0.486	0.477			
0.1				0.524	0.5	0.483	0.471	0.463			
0.2				0.5	0.479	0.464	0.453	0.447	0.443		
0.3					0.454	0.441	0.433	0.428	0.426		
0.4					0.427	0.416	0.409	0.405	0.405		
0.5					0.395	0.386	0.381	0.379	0.380		
0.6					0.357	0.351	0.347	0.347	0.349	0.355	
0.7						0.308	0.306	0.307	0.311	0.318	
0.8						0.255	0.254	0.256	0.261	0.268	
0.9						0.183	0.183	0.185	0.189	0.195	0.200
0.95						0.130	0.130	0.132	0.135	0.140	0.144

Table 1. Values of the first root p_1 of the Zak–Williams characteristic equation; see Equations (23) and (12).

results of [Romeo and Ballarini 1995] and with the results for several specific material pairs reported by [Cook and Erdogan 1972].

4. Stability analysis

Based on the analysis presented in Appendix A, we see that the Zak–Williams Equation (23) always possesses a single first root p_1 in the strip $0 \leq \operatorname{Re} p \leq 1$ which is simple and real. Furthermore, $0 < p_1 < 1/2$ when

$$\chi = \frac{\mu_1 \kappa_2}{\mu_2 \kappa_1}$$

the combination of elastic coefficients of both materials is less than unity.

Consequently, if $\chi < 1$ then, in view of Equation (26), $\lim_{\varepsilon \to 0} K_I = \infty$, and the crack is unstable in the vicinity of the interface. Similarly, when $\chi > 1$ then $1/2 < p_1 \leq 1$, $\lim_{\varepsilon \to 0} K_I = 0$, and the crack is stable. In this paper we consider only linear crack propagation. The stability of a crack with curvilinear path was investigated by [Gunnars et al. 1997]. We refer to the above combination of elastic coefficients "χ" as the crack stability factor (CSF). From the structure of the CSF we can see that the stability of the crack in the vicinity of an interface depends on the combination of Poisson ratios v_1 and v_2 as well as

$\alpha \setminus \beta$	−0.45	−0.4	−0.3	−0.2	−0.1	0	0.1	0.2	0.3	0.4	0.45
−0.95	0.330	0.406	0.466	0.487	0.492	0.487					
−0.9	0.352	0.425	0.481	0.5004	0.504	0.498					
−0.8		0.467	0.514	0.5285	0.529	0.521					
−0.7		0.513	0.549	0.5592	0.556	0.546					
−0.6		0.564	0.588	0.5926	0.587	0.574	0.555				
−0.5			0.630	0.6288	0.619	0.604	0.583				
−0.4			0.675	0.6678	0.655	0.636	0.613				
−0.3			0.724	0.7098	0.693	0.672	0.646				
−0.2			0.774	0.7546	0.734	0.711	0.683	0.651			
−0.1				0.8021	0.778	0.753	0.723	0.689			
0				0.8519	0.826	0.798	0.767	0.731			
0.1				0.9035	0.876	0.846	0.814	0.777			
0.2				0.9565	0.928	0.898	0.865	0.828	0.784		
0.3					0.982	0.953	0.921	0.884	0.840		
0.4					1.038	1.010	0.980	0.944	0.902		
0.5					1.095	1.070	1.042	1.009	0.970		
0.6					1.152	1.131	1.108	1.079	1.044	1.000	
0.7						1.194	1.176	1.153	1.125	1.088	
0.8						1.260	1.248	1.232	1.211	1.185	
0.9						1.333	1.326	1.318	1.307	1.292	1.283
0.95						1.376	1.373	1.369	1.363	1.354	1.349

Table 2. Values of $c(\alpha, \beta)$; see Equation (27).

the ratio of shear moduli μ_1/μ_2. Since the stress state in the problem under consideration is completely defined by the Dundurs parameters it is useful to exhibit the stability/instability zones in the plane (α, β); see Figure 2. It is clear that the stability condition $\alpha > 0$ employed by [Leguillon et al. 2000] holds true only for the specific case when $\beta = 0$.

The effect of the Poisson ratios ν_1 and ν_2 on crack stability at the interface is often overlooked. Typically the crack stability is determined on the basis of the shear moduli ratio only. If the crack exists in a more rigid material and approaches an interface with the softer material ($\mu_2 > \mu_1$ in Figure 1), it is regarded as unstable, see [Romeo and Ballarini 1995]. Consider, however, the case when the crack is in the more rigid material, $\mu_1/\mu_2 = 2/3$, $\nu_1 = 0.4$, and $\nu_2 = 0.2$. Calculation of the CSF for the plane strain case ($\kappa_s = 3 - 4\nu_s$, $s = 1, 2$) yields $\chi > 1$. Hence, in contrast to the conclusion based on $\mu_1/\mu_2 < 1$, the crack is stable. In the (α, β) plane the points corresponding to the material combinations possessing the above property are located within the lower sector generated by the lines $\alpha = \beta$ and $\alpha = -\beta$; see Figure 2. Examples of the corresponding engineering materials combinations can be identified using the data presented by [Suga et al. 1988].

As we noted at the beginning of the previous section, the stresses between the crack tip and the interface are non-zero only in the second problem taking part in the superposition. Their transform $\sigma(r, \pi)$ can
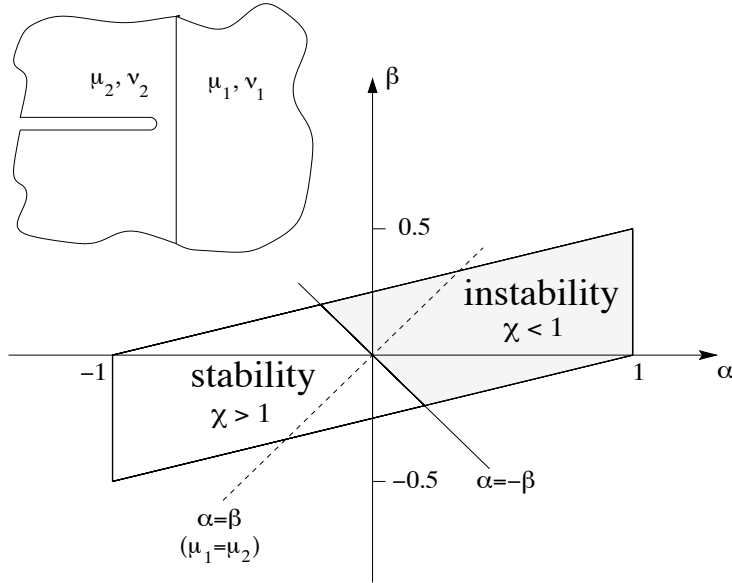
Figure 2. Crack stability and instability regions in the α, β plane. The dashed line corresponds to the equal shear moduli of the materials on both sides of the interface.

be determined in the same way we derived the asymptote in Equation (24). Hence,

$$\sigma_\theta(r, \pi) = \frac{1}{2\pi i} \int_{L_0} K^+(p) \sum_{k=1}^{\infty} \frac{Q(-p_k)}{(p + p_k) K^-(-p_k) N'(-p_k) h^{p_k}} r^{-p-1} dp \ .$$

After closing the integration path to the left of the contour L_0 we employ the residue theorem which leads to the formula for the stresses in front of the crack. In view of Equation (21) and using the nonscaled variables, we obtain

$$\sigma_\theta(R, \pi) = -\frac{1}{\pi \varepsilon} \sum_{n=1}^{\infty} \sum_{k=1}^{\infty} \frac{(-1)^n n \sin \pi p_k \ N(-n) \ K^-(-n)(R/\varepsilon)^{n-1}}{p_k(p_k - n) \ N'(-p_k) \ K^-(-p_k)(H/\varepsilon)^{p_k}} \ , \qquad 0 < R < \varepsilon \ . \tag{28}$$

The stress distribution between the crack tip and the interface is depicted in Figure 3. As an illustration, consider the aluminum-epoxy composite. The material parameters needed for the computations are provided in Table 3. The dashed curves represent the inverse square root asymptotes obtained from

Table 3. Material properties.

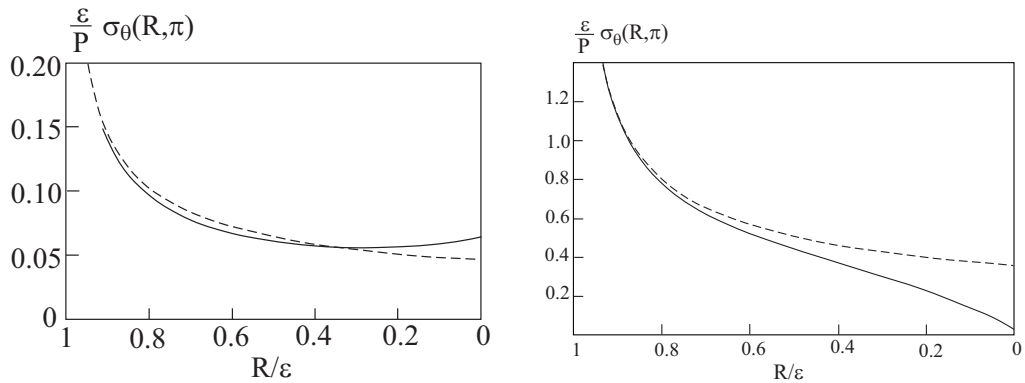|	Young modulus E (GPa)	Poisson ratio ν
Epoxy	3	0.345
Aluminum	70	0.333
Boron	380	0.2

Figure 3. Hoop stress distribution between the crack tip and the interface in the aluminum-epoxy composite for the crack located in the epoxy (left) and in the aluminum (right). The dashed lines denote the inverse square root asymptotes.

Equation (25) and correspond to the case of a homogeneous plane. In the first case (Figure 3, left) the crack is imbedded in the soft (epoxy) constituent and is stable ($\chi = 22.7 > 1$). As expected, the stresses the near tip are less than for a crack in a homogeneous plane. Somewhat surprisingly, however, the stresses near the interface increase and are nonmonotonic. The quantitative analysis of the results reveals that: (1) the inverse square root asymptote agrees well with the exact solution only within about 0.1ε from the crack tip; (2) within roughly 0.7ε the asymptote has the same trend as the exact solution; (3) the asymptote underestimates by approximately 30% the value of stress at the interface ($R = 0$), where the hoop stress reaches the local maximum. When the materials are reversed (Figure 3, right) the crack is located within the aluminum and is unstable ($\chi = 1/22.7$). In this case: (1) the inverse square root asymptote also agrees well with the exact solution within about 0.15ε from the crack tip; (2) however, the asymptote increasingly overestimates stresses as the distance from the crack tip grows, reaching about 30% at $R = 0.7\varepsilon$; and (3) it grossly overestimates the values of stresses near the interface ($R = 0$). The observed stress distributions agree with the data reported by [Wang and Stahle 1998] who investigated the crack approaching the interface by means of the semi-analytical dislocation approach.

The actual size of the K-dominance zone, which is proportional to ε, decreases for the crack approaching the interface. Thus at some point it becomes comparable to the fracture process zone of the cracked material. As a result, the standard fracture toughness criterion of crack propagation becomes invalid even for brittle materials and a nonasymptotic analysis of the stress field in the crack tip vicinity is required. This point is discussed in detail in [Ryvkin et al. 1995] and is illustrated in [Ryvkin 2000] in the problem of a crack close to a bimaterial interface. In the case of an unstable crack, which has no reason to stop after it begins to move for some finite value of ε, the above remark probably does not apply. The stable crack, on the other hand, may be arrested for vanishingly small ε. Consequently, the analysis of the complete stress distribution in front of a stable crack is of primary interest.

The influence of the elastic mismatch (the aluminum-epoxy and the boron-epoxy composites) on the stress distribution in front of a stable crack is illustrated in Figure 4.
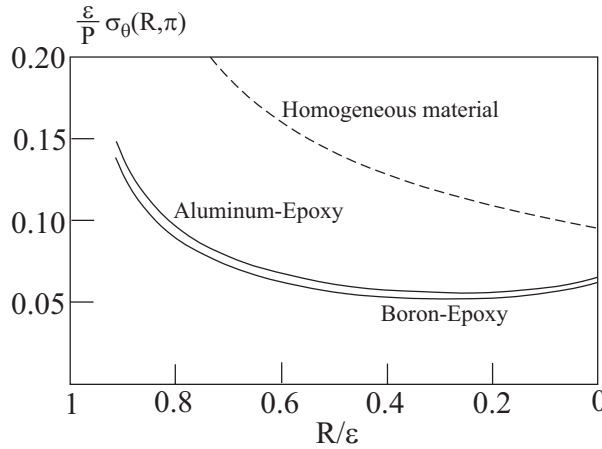
Figure 4. Stresses in front of the crack in the aluminum-epoxy and boron-epoxy composites. The dashed line is associated with the stresses in front of a crack in a homogeneous material.

For reference, the stress distribution for the crack in a homogeneous material is also shown by a dashed line. As expected, a greater mismatch of the materials leads to decrease in the stress. In spite of the fact that the stiffness of boron is greater than aluminum, the difference in stresses is nominal. This is attributable to the large mismatch between the epoxy and both of the above materials. Therefore the difference between them is of secondary importance and the bimaterial systems approach the limiting case of the epoxy half-plane bonded to a rigid substrate.

In order to examine the stress distribution on both sides of the interface, we need to derive the expression for the stress $\sigma(r, 0)$ in the uncracked material. In contrast to the stress $\sigma(r, \pi)$ here we have to superpose the stresses in both problems formulated in the beginning of the previous section. After some manipulation and employing the residue theorem, we obtain for $0 < r < 1$

$$\sigma_\theta(r, 0) = \frac{1}{\pi} \sum_{n=1}^{\infty} \sum_{k=1}^{\infty} \frac{(-1)^n n \sin \pi p_k \, U(-n) \, K^-(-n) r^{n-1}}{p_k(p_k - n) \, N'(-p_k) \, K^-(-p_k) h^{p_k}} \, ,$$

where

$$U(p) = (1 + \kappa_2)[\kappa_2(2p - 1) - 1 - 2p - \mu(1 + \kappa_1 - 2p + 2\kappa_1 p)].$$

The nonscaled expression is determined in a manner similar to Equation (28). The stresses in the ε vicinity of the interface in the aluminum-epoxy composite are depicted in Figure 5. As before, the dashed line corresponds to the crack in a homogeneous material.

In accord with the continuity of the hoop strain component, the stresses beyond the interface in the relatively stiff aluminum jump to a value higher than that in the epoxy. For some material combinations this phenomenon may lead to a new crack nucleation within the stiff constituent, see [Leguillon et al. 2000].

As noted above, the SIF vanishes in the case of a stable crack approaching the interface. However, this does not suggest that the stable crack can not reach the interface. In order to examine this opportunity, a
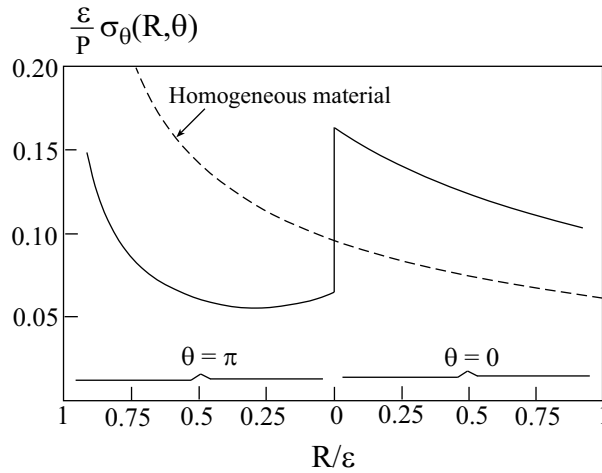
Figure 5. Stresses in the ε-vicinity of the interface.

critical stress-based criterion such as the Neuber–Novozhilov criterion [Neuber 1937; Novozhilov 1969] or the criterion indicated in [Cook and Erdogan 1972] needs to be employed rather than the fracture toughness criterion. After a crack has reached the interface, further crack propagation is defined by the competition between two possibilities: the penetration of the interface or deflection into it, see [He and Hutchinson 1989]. The need for a stress-based criterion is supported by the fact that the leading term in the expression given by Equation (28) for the stresses in front of a crack is proportional to ε^{p_1-1} and becomes unbounded when $\varepsilon \to 0$. Consequently, when the crack approaches the interface the stresses in the interface vicinity increase. Two opposite trends in the dependence of the stresses upon ε near the crack tip and near the interface are illustrated in Figure 6. Unlike the previous graphs, the coordinate system located at the crack tip is employed as shown in the insert.

Therefore the crack tip is associated with the left side of the graph and the crack propagation corresponds to the different positions of the interface denoted in the figure by the dashed lines. Since the results for several crack locations are depicted, the parameter employed for the length scale normalization here is H and not ε as it was previously. The stress distributions for three different distances between the crack tip and the interface ($\varepsilon/H = 0.1, 0.05$ and 0.02) are presented. The limiting values of stress at the interface are derived in an accurate manner from a simple formula given by the first term of the infinite sum in Equation (28). Thus,

$$\sigma_\theta(0, \pi) = \frac{1}{\pi\varepsilon} \frac{\sin \pi p_1 \ N(-1) \ K^-(-1)}{p_1(p_1 - n) \ N'(-p_1) \ K^-(-p_1)(H/\varepsilon)^{p_1}} .$$

These values are denoted in the figure by the circles. As the distance between the crack tip and the interface decreases, so does the stress singularity in the crack tip vicinity. On the other hand, the nonmonotonic stress behavior becomes more pronounced and the stresses near the interface increase, which at some point may lead to nucleation of a new microcrack located on the crack line and terminating at the interface.
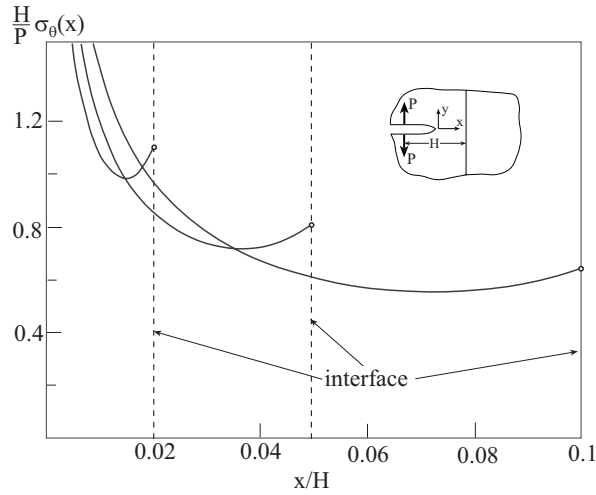
Figure 6. Stress distribution for the different distances between the tip of a stable crack and the interface.

The above approach is numerically very efficient. In order to reach less than one percent accuracy, 100 terms of the series in n and 3 terms of the series in k need to be taken into account. This is not surprising since, as it was noted, the series in k converges exponentially.

5. Conclusion

In this paper, we obtained a closed-form solution for the stress distribution in two perfectly bonded isotropic elastic half-planes with a fully imbedded semi-infinite crack orthogonal to the interface under Mode I loading by means of the Winner–Hopf–Jones method. The Green's functions for the stresses and the SIF are constructed using auxiliary problems solved in quadratures. The closed-form solution of the problem offers a way to express the result in a form convenient for computation. A quantitative characterization of the SIF for various combinations of elastic parameters via the function $c(\alpha, \beta)$ provides a practical tool for the solution of crack-interface interaction problems for arbitrarily distributed Mode I loading. The values of the function $c(\alpha, \beta)$ computed from the closed-form solution reported herein, when compared with those obtained previously by the numerical solution of singular integral equations [Romeo and Ballarini 1995], suggest an error in the later procedure.

In order to characterize the stability of a crack approaching the interface, we introduced a new *interface parameter*, χ, which is a simple combination of the shear moduli μ_s and the Poisson ratios ν_s ($s = 1, 2$) of the materials on both sides of the interface. The crack stability or instability in the vicinity of the interface is associated with a decrease or increase of the energy release rate, that is, SIF with $\varepsilon \to 0$. Since K_I behaves as $\varepsilon^{p_1 - 1/2}$, the crack stability or instability depends on p_1 being greater or less than 1/2. This result agrees with the former asymptotic investigations of the problem, but we established here for the first time the exact condition of crack stability in terms of material parameters. The interface parameter χ uniquely determines the sign of inequality for the first root p_1 of the Zak–Williams characteristic equation and thus indicates the asymptotic behavior of the SIF. An estimation of the interface parameter prior to

detailed computations may serve as a qualitative evaluation of the strength of the stress singularity in the vicinity of the interface.

It appears that the propagation of a stable crack cannot be predicted in the framework of the SIF approach. In this case the critical stress criterion can be employed in conjunction with the solution obtained.

Appendix A: Study of the first root of Zak–Williams characteristic equation

The dependence of the stress distribution and the SIF on the material properties in two perfectly bounded isotropic elastic half-planes with a crack approaching the interface is conventionally expressed in terms of the Dundurs parameters α and β.

$$\alpha = \frac{\mu(\kappa_1 + 1) - \kappa_2 - 1}{\mu(\kappa_1 + 1) + \kappa_2 + 1}, \qquad \beta = \frac{\mu(\kappa_1 - 1) - \kappa_2 + 1}{\mu(\kappa_1 + 1) + \kappa_2 + 1}.$$

The crack stability in the vicinity of the interface is determined by the value of the first root $p = p_1$ of the Zak–Williams characteristic equation [1963]. Specifically, the crack is stable when $1/2 < p_1 < 1$ or unstable when $0 < p_1 < 1/2$. In what follows we analyze the value of p_1 and the dependence of the crack stability on the material properties of both sides of the interface. The Zak–Williams equation can be presented in terms of the function N(p) in Equation (23). According to Equation (12) $N(p)$ can be explicitly written as

$$N(p) = 2(1 + \kappa_1)[(\mu + \kappa_2)\cos \pi p + 2(\mu - 1)p^2] - 2\kappa_1\mu^2 - (\kappa_1 - 1)(\kappa_2 - 1)\mu + \kappa_2^2 + 1. \quad (29)$$

Therefore it may be considered as a function of one complex variable p and three real variables κ_1, κ_2, and $\mu : N(p) \equiv N(\omega, p)$, $\omega = (\kappa_1, \kappa_2, \mu)$. Let us denote

$$p = \eta + i\xi, \ \eta = \operatorname{Re} p, \ \xi = \operatorname{Im} p; \quad N(p) = U(p) + iV(p), \ U(p) = \operatorname{Re} N(p), \ V(p) = \operatorname{Im} N(p). \quad (30)$$

The expressions of the material parameters through the Poisson ratios and shear moduli $\kappa_s = 3 - 4\nu_s$, $s = 1, 2$, and $\mu = \mu_2/\mu_1$ indicate the limits $1 < \kappa_s < 3$, $0 < \mu < \infty$. Consequently, we assume that $\omega \in \Omega$, where $\Omega = \{\omega : 1 < \kappa_s < 3, 0 < \mu < M\}$ is a 3–dimensional parallelepiped and M is an arbitrary large number. Furthermore, we define a rectangle domain $D = \operatorname{Re} p \in (0, 1)$, $\operatorname{Im} p \in (-q, q)$ in the complex plane with the boundary Γ. The barred symbols $\bar{\Omega}$ and $\bar{D}$ denote the closed sets and $\Omega \times D$ represents the Cartesian product.

Lemma 1. The function $N(\omega, p)$ does not vanish on the imaginary axis $\operatorname{Re} p = 0$ for any $\omega \in \bar{\Omega}$.

Proof. In view of Equations (29) and (30) we obtain

$$U(0) = \mu(1 + \kappa_1 + \kappa_2 + \kappa_1\kappa_2) + (\kappa_2 + 1)^2 > 0,$$

$$\frac{\partial U(i\xi)}{\partial \xi} = 2(1 + \kappa_1\mu)[\pi(\mu + \kappa_2)\sinh \pi\xi - 4(\mu - 1)\xi] \geq 2(1 + \kappa_1\mu)[\pi^2(\mu + \kappa_2)\xi - 4(\mu - 1)\xi]$$

$$= 2(1 + \kappa_1\mu)[(\pi^2 - 4)\mu + \kappa_2\pi^2 + 4]\xi \geq 0, \qquad \xi \geq 0.$$

Since $U(0) > 0$ and $\partial U(i\xi)/\partial \xi \geq 0$ for $\xi \geq 0$, the function $U(i\xi)$ increases monotonically for positive ξ and $U(i\xi) > 0$ for $\xi \geq 0$. From the evenness of function $U(i\xi)$ it follows that $N(i\xi) > 0$ for any ξ. $\square$

Lemma 2. The function $N(\omega, p)$, $\omega \in \bar{\Omega}$, does not vanish on the line $p = 1 + i\xi$ for any $\omega \in \bar{\Omega}$.

Proof. For $\mu \neq 1$ and $|\xi| > 0$ we have $V(1 + i\xi) = 8(1 + \kappa_1 \mu)(\mu - 1)\xi \neq 0$. Taking into account that $\kappa_1, \kappa_2 \in [1, 3]$, for $\mu = 1$ and $|\xi| \neq 0$ we the have

$$U(1 + i\xi) = -2(1 + \kappa_1)(1 + \kappa_2) \cosh \pi \xi - 2\kappa_1 - (\kappa_1 - 1)(\kappa_2 - 1) + \kappa_2^2 + 1 < -8 \cosh \pi \xi - 2 + \kappa_2^2 + 1 < 0.$$

For the case when $\xi = 0$, $\omega \in \bar{\Omega}$ we find $U(1) = \mu(1 + \kappa_1)(1 - 3\kappa_1) + (\kappa_2 - 1)^2 - 4 \leq \mu(1 + \kappa_2)(1 - 3\kappa_1) < 0$. Consequently, $N(1 + i\xi) \neq 0$ for all $\xi \in (-\infty, \infty)$.   □

Lemma 3. It is possible to find a positive number c defined by the following condition: the function $N(\omega, p)$, $\omega \in \hat{\Omega}$, is not vanishing on the segments Re $p \in [0, 1]$, Im $p = \pm q$ for any $q > c$.

Proof. The lower bound for c may be easily found by estimating the function $\cos \pi p$ by the first three terms of the Maclaurin series expansion in the rectangular domain $0 \leq \eta \leq 1$, $-c \leq \xi \leq c$.   □

Lemma 4. For the case when $\kappa_1 = \kappa_2$ and $\mu = 1$, function $N(\omega, p)$ has the only zero $p_1 = 1/2$ in the strip Re $p \in [0, 1]$.

Proof. For this case $N(\omega, p) = (1 + \kappa_1)^2 \cos \pi p$.   □

Theorem 1. The function $N(\omega, p)$, $\omega \in \bar{\Omega}$ has a single, simple and real zero in the strip $0 \leq$ Re $p \leq 1$.

Proof. For any $\omega \in \hat{\Omega}$ the function $N(\omega, p)$ of the complex variable p is analytic for $p \in D$, is continuous with its derivative on Γ, and, following Lemmas 1–3, does not vanish on this contour. Therefore, in accord with the principle of the argument, an integral along the closed contour Γ

$$I(\omega) = \frac{1}{2\pi i} \int_\Gamma \frac{N_p'(\omega, p)}{N(\omega, p)} dp \tag{31}$$

is equal to the total number (with regard to multiplicity) of zeros of the function $N(\omega, p)$ in D.

Changing the elastic parameters along some path in Ω, let us assume that for some point ω_* an r-order zero of the function $N(\omega, p)$ appears (or disappears) in D. Then the function $I(\omega)$ will have a finite r-units discontinuity at this point. However, the integrand in Equation (31) is continuous in $\bar{\Omega} \times \Gamma$ since the absolute values of its partial derivatives with respect to p and ω are bounded in this domain. Therefore the integral $I(\omega)$, $\omega \in \bar{\Omega}$ also represents a continuous function of ω.

The above contradiction leads to the conclusion that for any $\omega \in \Omega$ the function $N(\omega, p)$ has the same number of zeros in D, that is, $I(\omega) = const = n$. Since Lemma 4 implies that for $\omega = \omega_0 = (\kappa_1, \kappa_2, 1)$ there is the only simple zero is $p_1 = 1/2$, we then find that $n = 1$. Clearly this single zero can not become complex valued for some ω because in that case the conjugate number $\bar{p}_1$ also satisfies Equation (29).

Finally, since $q > 0$ is unbounded, the above result obtained for $p \in D$ holds for the entire strip $0 \leq$ Re $p \leq 1$.

Since for every $\omega \in \Omega$ corresponds some value of the first zero p_1 of the function $N(\omega, p)$, $(\omega, p) \in \bar{\Omega} \times \bar{D}$, we can consider an implicit function $p = f(\omega)$, $\omega \in \bar{\Omega}$. This function must fulfill the equation $N(\omega, p) = 0$, $(\omega, p) \in \hat{\Omega} \times \hat{D}$ and, in accord with Lemma 4, meet the condition $f(\omega_0) = 1/2$.   □

Remark 1. Theorem 1 can be now formulated as follows: The function $p = f(\omega)$, $\omega \in \bar{\Omega}$ exists, it is real valued, and it varies in a domain $P \subset (0, 1)$.

Remark 2. The function $N(\omega, p)$ and its derivative $\partial/\partial p[N(\omega, p)]$ do not vanish simultaneously in any point of the domain $\bar{\Omega} \times \bar{D}$.

Proof. The existence of such a point implies that function $N(\omega, p)$ has a multiple zero at this point, which violates Theorem 1. $\qquad\square$

Theorem 2. The implicit function $p = f(\omega)$, $\omega \in \bar{\Omega}$ defined by the equation $N(\omega, p) = 0$, $(\omega, p) \in \bar{\Omega} \times \bar{D}$ and condition $f(\omega_0) = 1/2$ exists. It is unique, continuous, and has continuous bounded partial derivatives.

Proof. In accord with Theorem 1 there exists a unique implicit function $p = f(\omega)$, $\omega \in \bar{\Omega}$ which is defined by a zero of the function $N(\omega, p)$ for a given ω. Since the partial derivatives of the function $N(\omega, p)$ of the first and second order in any bounded domain are bounded, function $N(\omega, p)$ and its derivative are continuous in the 4-dimensional parallelepiped $\bar{\Omega} \times [0, 1]$. Furthermore, following Remark 2, the functions $N(\omega, p)$ and $\partial/\partial p[N(\omega, p)]$ do not vanish simultaneously. The theorem of implicit functions then establishes that function $p = f(\omega)$ is continuous and its first derivatives

$$\frac{\partial p}{\partial \mu} = -\frac{\partial N(\omega, p)}{\partial \mu}\left[\frac{\partial N(\omega, p)}{\partial p}\right]^{-1}, \qquad \frac{\partial p}{\partial \kappa_s} = -\frac{\partial N(\omega, p)}{\partial \kappa_s}\left[\frac{\partial N(\omega, p)}{\partial p}\right]^{-1}, \qquad s = 1, 2 \quad (32)$$

exist and are continuous and bounded. $\qquad\square$

Lemma 5. Consider a surface S in Ω defined by the equation $\kappa_1\mu - \kappa_2 = 0$. Then every point $(\omega, 1/2)$, $\omega \in S$ from $\bar{\Omega} \times [0, 1]$ is zero of the function $N(\omega, p)$ and for the points with $\omega \bar{\subset} S$, $N(\omega, 1/2) \neq 0$.

Proof. The proof is obvious from the relation $N(\omega, 1/2) = (\kappa_2 - \kappa_1\mu)(\mu + \kappa_2)$. $\qquad\square$

Lemma 6. For arbitrary fixed $\kappa_1, \kappa_2 \in [1, 3]$ the function $p = f(\kappa_1, \kappa_2, \mu)$ represents a decreasing function of μ in the vicinity of the point $\mu_1 = \kappa_2/\kappa_1$.

Proof. In accord with Theorem 2, the partial derivatives of the function $N(\omega, p)$ in $\bar{\Omega} \times \bar{D}$ exist and are bounded. At the point $(\omega_1, 1/2)$, $\omega_1 = (\kappa_1, \kappa_2, \kappa_2\kappa_1^{-1})$, the partial derivatives are negative:

$$\frac{\partial N(\omega_1, 1/2)}{\partial \mu} = -\kappa_2(1 + \kappa_1) < 0\,,$$

$$\frac{\partial N(\omega_1, 1/2)}{\partial p} = 2(1 + \kappa_2)\kappa_1^{-1}[\pi(1 + \kappa_1)\kappa_2 - 2(\kappa_2 - \kappa_1)] < 2(1 + \kappa_2)\kappa_1^{-1}(4 - 2\pi) < 0\,.$$

Recalling Equation (32) we conclude that $\partial f(\omega_1)/\partial \mu < 0$ and the function $f(\omega)$ decreases with respect to μ at the point ω_1. The surface S separates the parallelepiped $\bar{\Omega}$ into two parts: $\bar{\Omega}^-$ for $\mu < \kappa_2\kappa_1^{-1}$ and $\bar{\Omega}^+$ for $\mu > \kappa_2\kappa_1^{-1}$. $\qquad\square$

Theorem 3. If $\omega \in \bar{\Omega}^+$, then $f(\omega) < 1/2$. If $\omega \in \bar{\Omega}^-$, then $f(\omega) > 1/2$.

Proof. Let us assume the opposite, that is, for some point $\omega_2 = (\kappa_1, \kappa_2, \mu)$ from $\bar{\Omega}^+$ $p_2 = f(\omega_2) \geq 1/2$. Lemma 5 states that the case of equality is impossible since $\omega_2 \notin S$, so we consider the case when $p_2 > 1/2$. We connect the points $\omega_1 = (\kappa_1, \kappa_2, \kappa_2\kappa_1^{-1})$ and ω_2 by a line segment γ and consider the function $p = f(\omega) = \varphi(\mu)$ on γ. By Lemma 6 this function is deceasing in the vicinity of the point ω_1. By Lemma 5 $\varphi(\mu_1) = 1/2$. Consequently, there is a point μ_3 where $p_3 = \varphi(\mu_3) < 1/2$. Continuous in accord with Theorem 2, the function $\varphi(\mu)$ takes on the segment (μ_3, μ_2) all the intermediate values

between p_3 and p_2. Therefore the point $\mu_4 \in (\mu_3, \mu_2)$ exists where $\varphi(\mu_4) = 1/2$. But this results in a contradiction with Lemma 5 since the point $(\kappa_1, \kappa_2, \mu_4) \in \bar{\Omega}^+$ is not located on S and cannot be a zero of the function $N(\omega, 1/2)$. The proof of the second part of the theorem is carried out in a similar manner. $\qquad \square$

Summary. Initially we sought zeros of the function $N(\omega, p)$ in the 5-dimensional domain $\Omega \times D$ characterized by five real valued parameters two of which (μ and ξ) are unbounded. Answering the question on the existence of zeros and their number, Theorem 1 reduced substantially the range of possible locations for p_1. Theorem 2 and Lemma 5 provided the foundation for developing a simple iterative procedure with respect to μ based on the continuous dependence of p_1 upon all the parameters $\omega(\kappa_1, \kappa_2, \mu)$ and the known initial value $p_1 = 1/2$ for $\mu = \kappa_2 \kappa_1^{-1}$. Finally, Theorem 3 allows us to answer the question of whether the crack will be stable ($\mu < \kappa_2 \kappa_1^{-1}$, $\chi > 1$, $p_1 > 1/2$) or unstable ($\mu > \kappa_2 \kappa_1^{-1}$, $\chi < 1$, $p_1 < 1/2$) for $\varepsilon \to 0$ a priori, without any calculations. We only need to know the elastic parameters of the composite body, namely, the ratio $\mu = \mu_2/\mu_1$ and $\kappa_s = 3 - 4\nu_s$.

Acknowledgements

Homage

On September 5, 2002, after a long fight with cancer, Professor Boris M. Nuller passed away.

Born in 1934, Boris Nuller survived the winter of 1941 in Leningrad under the siege. He received his Ph.D. and D.Sci. degrees from Leningrad Polytechnic Institute, and during the last few years served as head of the Mathematics Department of the Leningrad Forestry Academy. Publishing over 200 scientific papers in his lifetime, many of which found industrial application, Professor Nuller dedicated his exceptional mathematical talent to applied mechanics. He developed a method of piecewise homogeneous solutions for problems with mixed boundary conditions, improved the methods of solution of Gilbert–Riemann and Wiener–Hopf functional equations, and advanced the technique of discrete Fourier transforms for domains possessing cyclic or translational symmetry. Among his numerous contributions are solutions of various contact problems related mainly to fracture mechanics, the development of nonlinear poro-elasticity and a mathematical model of cutting.

Professor Nuller's friendship, his commitment to research, his creativity, and his insight into the problems of mathematical physics will be missed.

References

[Atkinson 1975] C. Atkinson, "On the stress intensity factors associated with cracks interacting with an interface between two elastic media", *Int. J. Eng. Sci.* **13**:5 (1975), 489–504.

[Cook and Erdogan 1972] T. S. Cook and F. Erdogan, "Stress in bonded materials with a crack perpendicular to the interface", *Int. J. Eng. Sci.* **10**:8 (1972), 677–697.

[Erdogan and Biricikoglu 1973] F. Erdogan and V. Biricikoglu, "Two bonded half-planes with a crack going through the interface", *Int. J. Eng. Sci.* **11**:7 (1973), 745–766.

[Gakhov 1966] F. D. Gakhov, *Boundary value problems*, Pergamon Press, London, UK, 1966.

[Gunnars et al. 1997] J. Gunnars, P. Stahle, and T. C. Wang, "On crack path stability in a layered material", *Comput. Mech.* **19**:6 (1997), 545–552.

[He and Hutchinson 1989] M.-Y. He and J. W. Hutchinson, "Crack deflection at an interface between dissimilar elastic materials", *Int. J. Solids Struct.* **25**:9 (1989), 1053–1067.

[Khrapkov 1968] A. A. Khrapkov, "First fundamental problem for a piecewise-homogeneous plane with a slit perpendicular to the line of separation", *J. Appl. Math. Mech.* **32**:4 (1968), 666–678.

[Leguillon et al. 2000] D. Leguillon, C. Lacroix, and E. Martin, "Interface debonding ahead of a primary crack", *J. Mech. Phys. Solids* **48**:10 (2000), 2137–2161.

[Neuber 1937] H. Neuber, *Kerbspannungslehre*, Springer, Berlin, Germany, 1937.

[Noble 1958] B. Noble, *Method based on the Wiener-Hopf technique for solution of partial differential equations*, Pergamon Press, Oxford, UK, 1958.

[Novozhilov 1969] V. V. Novozhilov, "On a necessary and sufficient criterion for brittle strength", *J. Appl. Math. Mech.* **33**:2 (1969), 201–210.

[Nuller 1976] B. M. Nuller, "Contact problem for an elastic wedge reinforced by a bar of uniform resistance", *Sov. Phys. Doklady* **20** (1976), 789–790.

[Nuller et al. 2001] B. Nuller, M. Ryvkin, A. Chudnovsky, J. W. Dudley, and G. K. Wong, "Crack interaction with an interface in laminated elastic media", pp. 289–296 in *Proceedings: Rock Mechanics in the National Interest*, edited by D. Elsworth and et. al, Washington, DC, July 2001.

[Romeo and Ballarini 1995] A. Romeo and R. Ballarini, "A crack very close to a bimaterial interface", *J. Appl. Mech.* (*Trans. ASME*) **62** (1995), 614–619.

[Ryvkin 2000] M. Ryvkin, "K–dominance zone for a semi–infinite mode I crack in a sandwich composite", *Int. J. Solids Struct.* **37**:35 (2000), 4825–4840.

[Ryvkin et al. 1995] M. Ryvkin, L. Slepyan, and L. Banks-Sills, "On the scale effect in the thin layer delamination problem", *Int. J. Fract.* **71**:3 (1995), 247–271.

[Suga et al. 1988] T. Suga, G. Elssner, and S. Schmauder, "Composite parameters and mechanical compatibility of material joints", *J. Compos. Mater.* **22**:10 (1988), 917–934.

[Wang and Stahle 1998] T. C. Wang and P. Stahle, "Stress state in front of a crack perpendicular to bimaterial interface", *Eng. Fract. Mech.* **59**:4 (1998), 471–485.

[Zak and Williams 1963] A. R. Zak and M. L. Williams, "Crack point stress singularities at a bi-material interface", *J. Appl. Mech.* (*Trans. ASME*) **30** (1963), 142–143.

BORIS NULLER: Deceased 5 Sep 2002
Department of Applied Mathematics, Kirov Academy of Wood Technology, St. Petersburg 195220, Russia

MICHAEL RYVKIN: arikr@eng.tau.ac.il
School of Mechanical Engineering, Iby and Aladar Fleischman Faculty of Engineering, Tel Aviv University, Tel Aviv 69978, Israel

ALEXANDER CHUDNOVSKY: achudnov@uic.edu
Department of Civil and Materials Engineering, The University of Illinois at Chicago, 842 West Taylor Street, Chicago, Illinois 60607-7023, United States